Magnetic proximity-enhanced Curie temperature of Cr-doped Bi_2Se_3 thin films

A. A. Baker,[1,2] A. I. Figueroa,[1] K. Kummer,[3] L. J. Collins-McIntyre,[2] T. Hesjedal,[2,4] and G. van der Laan[1,*]

[1]*Magnetic Spectroscopy Group, Diamond Light Source, Didcot OX11 0DE, United Kingdom*

[2]*Department of Physics, Clarendon Laboratory, University of Oxford, Oxford OX1 3PU, United Kingdom*

[3]*European Synchrotron Radiation Facility, BP 220, F-38043 Grenoble Cedex, France*

[4]*Diamond Light Source, Didcot OX11 0DE, United Kingdom*

(Received 24 April 2015; published 11 September 2015)

We report a study on the transition temperature T_C of Cr-doped topological insulator thin films, where an increase in the ferromagnetic onset can provide a pathway towards low-power spintronics in the future. Arrott plots, measured by surface-sensitive x-ray magnetic circular dichroism at the Cr $L_{2,3}$ edge as a function of field at various low temperatures, give a $T_C \approx 7$ K for the pristine surface. This is comparable to the bulk value of the film, which means that there is no indication that the spontaneous magnetization is different near the surface. Evaporation of a thin layer of Co onto the pristine surface of the *in-situ* cleaved sample increases the ordering temperature near the surface to ∼19 K, while in the bulk it rises to ∼10 K. X-ray absorption spectroscopy shows that Cr enters the Bi_2Se_3 host matrix in a divalent state, and is unchanged by the Co deposition. These results demonstrate a straightforward procedure to increase the transition temperature of doped topological insulators.

DOI: 10.1103/PhysRevB.92.094420 PACS number(s): 75.30.Hx, 78.70.Dm, 75.70.Cn, 73.61.Ng

Introduction. Topological insulators (TIs) [1,2] have gained strong interest as a new class of materials with fascinating yet exotic physics [3]. TIs host a gapless topological surface state (TSS) which exhibits a Dirac-cone-like dispersion. The topological surface state is protected by time-reversal symmetry (TRS). Magnetically doped TIs are host to a wide variety of exotic physical effects, perhaps most notably the recently confirmed quantum anomalous Hall effect (QAHE) [4], which requires the breaking of the TRS through the opening of a gap around the Dirac point [5]. Furthermore, such magnetically doped TIs offer extremely high spin-orbit torques, indicating great potential for spintronic devices [6].

The application of an external magnetic field or doping with magnetic impurities, e.g., transition-metal [7,8] or rare-earth [9,10] atoms, has been shown to break TRS in a TI. Mn doping of $(Bi,Sb)_2(Se,Te)_3$ has been initially a promising route [7], and magnetic proximity coupling through a deposited Fe overlayer has been shown to lead to an increased Curie temperature T_C [11]. Nevertheless, the QAHE was not observed in Mn-doped material, probably also because an increasing interstitial incorporation of Mn is observed with increasing doping concentration [12]. Cr remains the most promising dopant to achieve the QAHE [13], as it incorporates substitutionally on the Bi site [14] and leads to long-range ferromagnetic order at ∼8.5 K [15]. Recently, it has been shown that TIs proximity coupled to a ferrimagnetic insulator show an increased T_C [16], suggesting the great potential of interface engineering to improve their magnetic properties. Depositing an elemental ferromagnet on the surface of a highly crystalline TI is an attractive prospect, as it removes the complication of substrate effects or the introduction of epitaxial strain.

Recently, magnetic ordering at relatively high temperatures has been reported for doped TIs, such as up to 110 K for Mn:Bi_2Se_3 [17], but such measurements were performed under an applied magnetic field. However, the real transition temperature is not always easy to determine experimentally, since it is defined only in zero applied field. Even in the case of a perfectly accurate experiment, it is necessary to make the sample a single magnetic domain and to align all moments along the applied field. This sometimes requires rather large fields.

In this paper we use x-ray magnetic circular dichroism (XMCD) from an *in-situ* cleaved Cr:Bi_2Se_3 epitaxial thin film to study the structural and magnetic properties of the material in the cleanest possible state. Measuring the unoxidized interior of the film, we show unequivocally that Cr enters the host matrix as nominally Cr^{2+}, matching very closely the calculated multiplet structure of the spectra. Using the method of Arrott plots [18], where the isothermal magnetization is measured by XMCD as a function of field, we find a T_C of (7 ± 1) K, comparable to previous bulk-sensitive magnetometry measurements on the same films [15]. After *in-situ* evaporation of a ferromagnetic thin film of Co onto the cleaved surface at low temperatures, we find a clean interface with no evidence of alloying or any distortion of the XMCD spectra. The T_C of the Cr:Bi_2Se_3 underneath the Co is increased to (19 ± 1) K through the proximity effect, demonstrating that such interface effects can be used to boost the magnetic performance of magnetically doped TI thin films.

Experimental. Molecular beam epitaxy (MBE) was used to grow Cr-doped Bi_2Se_3 thin films of ∼100-nm thickness on *c*-plane sapphire substrates. The Cr concentration was adjusted via the Cr:Bi flux ratio, while supplying Se at a 10 times higher rate. The growth rate was ∼0.9 nm/min at a growth temperature of 300°C. For a detailed description of the growth procedure, see Ref. [15].

The structural properties of the films were characterized using x-ray diffraction (XRD). The films are of high crystalline quality and free of secondary phases [15] and Cr clusters [14]. The *c*-axis lattice constant remains virtually unchanged for the doped films as compared to Bi_2Se_3, supporting the finding of substitutional doping, obtained from extended x-ray absorption fine structure (EXAFS) [14]. The dopant concentration was calibrated using Rutherford back-scattering

*gerrit.vanderlaan@diamond.ac.uk

spectrometry (RBS) to be 4.6 at.% Cr for the investigated sample. The samples are ferromagnetic with a coercive field of 10 mT at 2 K and $T_C \approx 8.5$ K, as determined by the dip in the first derivative of the temperature dependent magnetization, $\partial M/\partial T$, measured by superconducting quantum interference device (SQUID) magnetometry [15]. The electric conductivity of the film is n type with a sheet carrier density of $n = -3.16 \times 10^{19}$ cm^{-3} at 5 K.

XMCD measurements were performed on beamline ID32 of the European Synchrotron Radiation Facility (ESRF), Grenoble, and beamline I10 at the Diamond Light Source, Oxfordshire. X-ray absorption spectroscopy (XAS) at the Cr and Co $L_{2,3}$ edges was detected in bulk-sensitive fluorescence yield (FY) mode and in total-electron-yield (TEY) mode, which is surface sensitive with a probing depth of 3 to 5 nm [19]. The XMCD was obtained as the difference between two XAS spectra recorded with the helicity vector antiparallel and parallel to the applied magnetic field ($\mu^- - \mu^+$), where μ is the absorption coefficient. Measurements were performed at grazing incidence (20°); the surface normal of the sample is along the c axis.

After *in-situ* cleaving and measurements on the pristine surface, a thin layer of ferromagnetic Co was evaporated from an electron-beam evaporator mounted in the XAS measurement chamber. The sample was kept at 10 K during this process to inhibit reactions between the incident Co atoms and the clean sample surface. Base pressure during evaporation was $<1 \times 10^{-9}$ Torr. XMCD measurements were performed at regular intervals during the deposition to check line shape and remanent magnetization. In this way the thickness of the Co layer can be estimated at ~3 nm.

Results. Figure 1 shows the Cr $L_{2,3}$ XAS and XMCD measured in TEY for as-grown and as-cleaved samples, together with calculated spectra for divalent Cr. There is an extra peak structure around 577.5 eV in the XAS for the as-grown sample, due to trivalent Cr arising from surface oxidation. After sample cleaving this second peak has completely disappeared. The same effect is observed in the XMCD.

Theoretical spectra were calculated using atomic multiplet theory, in which spin-orbit and electrostatic interactions are treated on equal footing, including crystal-field interaction and charge hybridization [20,21]. As we reported in Ref. [14], the spectra for bulk Cr:Bi_2Se_3 (taken with bulk-sensitive fluorescence yield detection) agree well with hybridized Cr states of 70% d^4 and 30% d^3 character in an octahedral crystal field.

Thus the Cr has nominally a divalent state, which seems remarkable as it substitutionally replaces Bi^{3+}. However, the Cr d band has a strong hybridization with the Se p band, which are located just above and below the Fermi level. The mixing between these electronic states is increased by the contraction of the Se atoms towards the Cr atom, compared to the undisturbed Se–Bi distance. The electronic charge is redistributed within the Cr–Se bonds, so that it does not contribute to the free carrier concentration [14].

Figure 1 shows that the cleaved sample gives an excellent agreement with the calculated spectra for nominal Cr^{2+}. This demonstrates unequivocally that Cr enters the host Bi_2Se_3 matrix in the Cr^{2+} valency, sitting substitutionally on the Bi site. Since the line shape is in agreement with measurements

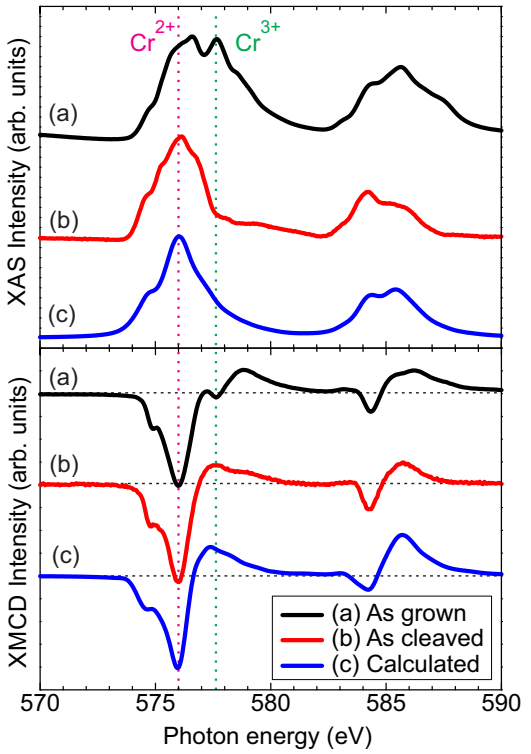

FIG. 1. (Color online) Cr $L_{2,3}$ XAS (upper panel) and XMCD (lower panel) measured in TEY for (a) as-grown (black) and (b) as-cleaved (red) Cr:Bi_2Se_3, and (c) calculated multiplet structure for nominally Cr^{2+} dopants (blue). The pronounced difference between the pristine surface obtained by cleaving and the oxidized surface of the as-grown sample indicates an additional Cr^{3+} contribution in the latter. The dotted vertical lines mark the photon energies of the two Cr valencies.

taken with bulk-sensitive fluorescence yield, the Cr electronic structure near the cleaved surface is the same as in the bulk.

Figure 2(a) shows the XAS and XMCD for the thin Co layer deposited onto the cleaved sample. The spectra show no evidence of alloying between Co and the underlying sample. Furthermore, the XMCD of the Cr in the film beneath [Fig. 2(b)] is unchanged from the as-cleaved spectrum. Thus the Co overlayer does not alter the chemical state of the Cr atoms.

Since the coercive field of ferromagnetically doped TIs is typically very small (10 mT at 2 K) [15], it is difficult to determine T_C by monitoring the closure of the loop opening in the XMCD hysteresis, measured using a superconducting magnet. We provide example magnetization and inverse susceptibility ($1/\chi$) measurements in the Supplemental Material to illustrate the problems of these approaches [22]. Instead, a more sensitive and accurate measurement is provided by the Arrott-plot criterion [18]. Minimization of the free energy in the Landau description of the magnetization leads to [23]

$$H/M = a(T - T_C) + bM^2, \tag{1}$$

where M is the magnetization, H is the applied field, T is the temperature, and a and b are constants. Rearrangement gives

$$M^2 = A(H/M) + B(T - T_C), \tag{2}$$

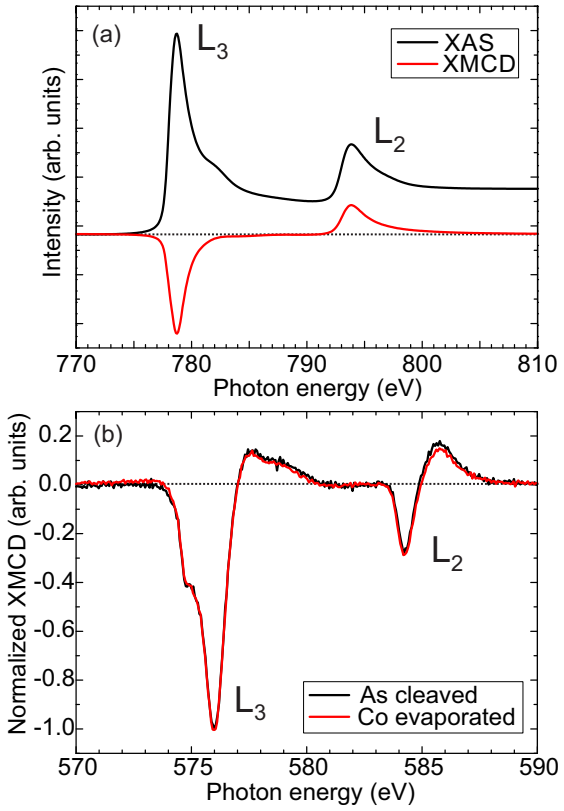

FIG. 2. (Color online) (a) Co $L_{2,3}$ XAS and XMCD for the thin layer of Co, grown on top of the cleaved Cr:Bi_2Se_3 thin film, measured in TEY at 10 K in a 0.5 T field. The clean, metallic line shapes indicates that no significant intermixing or alloying has taken place. (b) Normalized Cr $L_{2,3}$ XMCD at 10 K in an 8 T field taken before (black curve) and after (red curve) deposition of the Co layer, scaled to matching peak heights at L_3. It can be seen that the character of the Cr dopants is not affected by the addition of the ferromagnetic overlayer, only the magnetic ordering temperature is enhanced.

where $A = 1/b$ and $B = -a/b$. Arrott plots are obtained by plotting the isotherms of $M(H)$ and H as a function of M^2 vs H/M, which according to Eq. (2) should yield straight lines. However, disordered systems with a distribution of exchange coupling strengths can give rise to a bending of the curves, introducing additional complications [24,25]. In this case one must consider only the high-field region of the isotherms, which are presumed to be linear and parallel.

The intercept of the isotherms with the H/M axis (i.e., where $M^2 = 0$) is positive (negative) for $T > T_C$ ($T < T_C$). Hence, T_C is equal to that temperature for which the intercept is zero. The spontaneous magnetization M_s, i.e., the magnetization in zero applied field, is obtained from Eq. (2) as $M_s^2 = B(T - T_C)$.

Figures 3(a) and 3(b) show Arrott plots for the sample as-cleaved and with the Co overlayer, respectively. We use the background-corrected Cr L_3 XMCD asymmetry, $(\mu^- - \mu^+)/(\mu^- + \mu^+)$, which is directly proportional to M. As would be expected, the ferromagnetic transition is second order. By fitting parallel straight lines to the high-field regions (forcing the gradient of all lines to the same value), we obtain the H/M intercepts collected in Fig. 3(c). The zero point of this

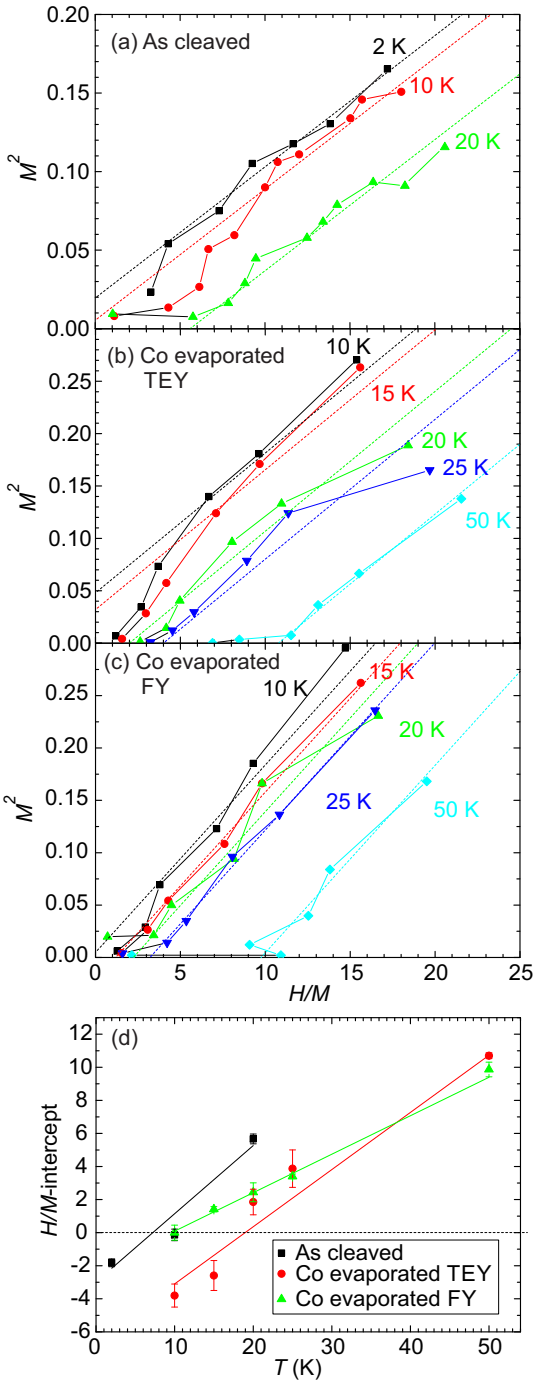

FIG. 3. (Color online) Arrott plots for (a) as-cleaved sample and (b),(c) same sample after evaporating a thin layer of Co on top measured with surface-sensitive TEY and bulk-sensitive FY, respectively. Plotted (in arbitrary units) are the isothermal variations of M^2 as a function of H/M, where H is the applied field and M is the magnetization as measured by the XMCD asymmetry of the Cr L_3 peak. Solid lines are a guide to the eye only. Dashed lines are linear fits to the high-field region of each isotherm. Panel (d) shows the H/M intercepts of the linear fits from panels (a), (b), and (c). The temperature at which the intercept goes through zero gives the T_C, which is (7 ± 1) K for the as-cleaved sample, which at the surface increases to (19 ± 1) K in the presence of the Co overlayer. However, FY gives $T_C = (10 \pm 1)$ K, which indicates that the enhancement of T_C is not homogeneous throughout the film.

intercept gives $T_C = (7 \pm 1)$ K for the as-cleaved sample, in close agreement with previous magnetometry measurements on these samples [15]. In contrast, with the Co overlayer the underlying film shows an increased T_C of (19 ± 1) K, more than twice that of the as-cleaved film. Intriguingly, measurements performed using FY lead to a measured T_C of (10 ± 1) K.

Discussion. It is important to note that the determination of magnetic properties from Arrott plots should ideally be performed with the use of critical exponents to transform the raw data [24]. Due to the time-consuming nature of XMCD measurements compared to conventional magnetometry we were not able to gather sufficient data points to determine these coefficients. The curvature of our Arrott plots is typical for such systems arising from magnetic disorder [25,26]. XMCD Arrott plots have only been sparsely reported [27]; however, this technique offers the great advantage of allowing independent determination of the magnetic behavior of different elements, enabling one to distinguish between different layers [19].

For the surface region of the as-cleaved sample the XMCD gives a T_C that is close to the value reported for the bulk of the film [15]. This is remarkable, as it means that the topological surface state has little influence on the T_C. It shows there is no additional spontaneous magnetization at the surface of the TI. However, the difference between surface-sensitive TEY and bulk-sensitive FY in the presence of a Co overlayer demonstrates that the proximity effect is of limited range. Since the as-cleaved data showed no enhancement of T_C at the surface, the apparent differing values given by TEY and FY likely arise from the short ranged exchange interaction with the ferromagnetic Co overlayer. This finding can be useful for the development of new physical models of Cr-doped Bi_2Se_3 and their use in, e.g., spintronic devices [6].

The results are important as they demonstrate a simple procedure through which T_C can be enhanced in ferromagnetically doped TIs. Putative device applications for this materials class are currently hindered by the requirement of extremely low operating temperatures, so any mechanism by which the ferromagnetic ordering temperature can be enhanced is of key interest.

Conclusion. We have performed x-ray absorption studies of the magnetic state of single-crystalline Cr:Bi_2Se_3 thin films, observing the onset of ferromagnetic order at ~7 K. The pristine surface shows a similar T_C as the bulk, meaning that there is no significant increase in the spontaneous magnetization at the surface of the TI. The T_C is more than doubled by depositing a thin layer of ferromagnetic Co, a significant gain for such a simple procedure. Comparison of TEY and FY measurements shows that this enhancement is most pronounced in the vicinity of the Co overlayer, with a smaller increase in T_C in the bulk of the film. Furthermore, spectroscopy measurements on as-cleaved samples demonstrate close agreement with calculations, confirming the presence of nominally Cr^{2+} dopants. It is hoped that these observations will provide a step towards low-power applications of TIs in spintronic devices in the near future.

Acknowledgments. Beam time awarded on ID32 at the ESRF (Proposal No. HC-1282) and on I10 at the Diamond Light Source (Proposal No. SI-10207) are acknowledged. T.H. acknowledges the John Fell Oxford University Press (OUP) Research Fund. A.A.B. was supported by Diamond Light Source and together with L.J.C.M. by EPSRC through Doctoral Training Awards.

[1] L. Fu, C. L. Kane, and E. J. Mele, Topological Insulators in Three Dimensions, Phys. Rev. Lett. **98**, 106803 (2007).

[2] B. A. Bernevig, T. L. Hughes, and S.-C. Zhang, Quantum spin Hall effect and topological phase transition in HgTe quantum wells, Science **314**, 1757 (2006).

[3] R. Yu, W. Zhang, H.-J. Zhang, S.-C. Zhang, X. Dai, and Z. Fang, Quantized anomalous Hall effect in magnetic topological insulators, Science **329**, 61 (2010).

[4] C.-Z. Chang, J. Zhang, X. Feng, J. Shen, Z. Zhang, M. Guo, K. Li, Y. Ou, P. Wei, L.-L. Wang, Z.-Q. Ji, Y. Feng, S. Ji, X. Chen, J. Jia, X. Dai, Z. Fang, S.-C. Zhang, K. He, Y. Wang, L. Lu, X.-C. Ma, and Q.-K. Xue, Experimental observation of the quantum anomalous Hall effect in a magnetic topological insulator, Science **340**, 167 (2013).

[5] Y. L. Chen, J.-H. Chu, J. G. Analytis, Z. K. Liu, K. Igarashi, H.-H. Kuo, X. L. Qi, S.-K. Mo, R. G. Moore, D. H. Lu, M. Hashimoto, T. Sasagawa, S. C. Zhang, I. R. Fisher, Z. Hussain, and Z. X. Shen, Massive Dirac fermion on the surface of a magnetically doped topological insulator, Science **329**, 659 (2010).

[6] Yabin Fan, Pramey Upadhyaya, Xufeng Kou, Murong Lang, So Takei, Zhenxing Wang, Jianshi Tang, Liang He, Li-Te Chang, Mohammad Montazeri *et al.*, Magnetization switching through giant spin–orbit torque in a magnetically doped topological insulator heterostructure, Nat. Mater. **13**, 699 (2014).

[7] C. Niu, Y. Dai, M. Guo, W. Wei, Y. Ma, and B. Huang, Mn induced ferromagnetism and modulated topological surface states in Bi_2Te_3, Appl. Phys. Lett. **98**, 252502 (2011).

[8] M. D. Watson, L. J. Collins-McIntyre, L. R. Shelford, A. I. Coldea, D. Prabhakaran, S. C. Speller, T. Mousavi, C. R. M. Grovenor, Z. Salman, S. R. Giblin, G. van der Laan, and T. Hesjedal, Study of the structural, electric and magnetic properties of Mn-doped Bi_2Te_3 single crystals, New J. Phys. **15**, 103016 (2013).

[9] S. Li, S. E. Harrison, Y. Huo, A. Pushp, H. T. Yuan, B. Zhou, A. J. Kellock, S. S. P. Parkin, Y.-L. Chen, T. Hesjedal, and J. S. Harris, Magnetic properties of gadolinium substituted Bi_2Te_3 thin films, Appl. Phys. Lett. **102**, 242412 (2013).

[10] S. E. Harrison, L. J. Collins-McIntyre, S. Li, A. A. Baker, L. R. Shelford, Y. Huo, A. Pushp, S. S. P. Parkin, J. S. Harris, E. Arenholz, G. van der Laan, and T. Hesjedal, Study of Gd-doped Bi_2Te_3 thin films: Molecular beam epitaxy growth and magnetic properties, J. Appl. Phys. **115**, 023904 (2014).

[11] I. Vobornik, U. Manju, J. Fujii, F. Borgatti, P. Torelli, D. Krizmancic, Y. S. Hor, R. J. Cava, and G. Panaccione, Magnetic proximity effect as a pathway to spintronic applications of topological insulators, Nano Lett. **11**, 4079 (2011).

[12] L. J. Collins-McIntyre, M. D. Watson, A. A. Baker, S. L. Zhang, A. I. Coldea, S. E. Harrison, A. Pushp, A. J. Kellock, S. S. P. Parkin, G. van der Laan, and T. Hesjedal, X-ray magnetic spectroscopy of MBE-grown Mn-doped Bi_2Se_3 thin films, AIP Adv. **4**, 127136 (2014).

[13] J. Zhang, C. Z. Chang, P. Tang, Z. Zhang, X. Feng, K. Li, L. L. Wang, X. Chen, C. Liu, W. Duan, K. He, Q. K. Xue, X. Ma, and Y. Wang, Topology-driven magnetic quantum phase transition in topological insulators, Science **339**, 1582 (2013).

[14] A. I. Figueroa, G. van der Laan, L. J. Collins-McIntyre, S.-L. Zhang, A. A. Baker, S. E. Harrison, P. Schönherr, G. Cibin, and T. Hesjedal, Magnetic Cr doping of Bi_2Se_3: Evidence for divalent Cr from x-ray spectroscopy, Phys. Rev. B **90**, 134402 (2014).

[15] L. J. Collins-McIntyre, S. E. Harrison, P. Schönherr, N.-J. Steinke, C. J. Kinane, T. R. Charlton, D. Alba-Venero, A. Pushp, A. J. Kellock, S. S. P. Parkin, J. S. Harris, S. Langridge, G. van der Laan, and T. Hesjedal, Magnetic ordering in Cr-doped Bi_2Se_3 thin films, Europhys. Lett. **107**, 57009 (2014).

[16] W. Q. Liu, L. He, Y. B. Xu, K. Murata, M. C. Onbasli, M. Lang, N. J. Maltby, S. Li, X. Wang, C. A. Ross, P. Bencok, G. van der Laan, R. Zhang, and K. L. Wang, Enhanced magnetic ordering in Cr-doped Bi_2Se_3 using high-T_C ferrimagnetic insulator, Nano Lett. **15**, 764 (2015).

[17] S.-Y. Xu, M. Neupane, C. Liu, D. M. Zhang, A. Richardella, L. A. Wray, N. Alidoust, M. Leandersson, T. Balasubramanian, J. Sánchez-Barriga, O. Rader, G. Landolt, B. Slomski, J. H. Dil, J. Osterwalder, T.-R. Chang, H.-T. Jeng, H. Lin, A. Bansil, N. Samarth, and M. Z. Hasan, Hedgehog spin texture and Berry's phase tuning in a magnetic topological insulator, Nat. Phys. **8**, 616 (2012).

[18] A. Arrott, Criterion for ferromagnetism from observations of magnetic isotherms, Phys. Rev. **108**, 1394 (1957).

[19] G. van der Laan and A. I. Figueroa, X-ray magnetic circular dichroism—A versatile tool to study magnetism, Coord. Chem. Rev. **277-278**, 95 (2014).

[20] G. van der Laan, Hitchhiker's guide to multiplet calculations, Lect. Notes Phys. **697**, 143 (2006).

[21] G. van der Laan and B. T. Thole, Strong magnetic x-ray dichroism in $2p$ absorption spectra of $3d$ transition-metal ions, Phys. Rev. B **43**, 13401 (1991).

[22] See Supplemental Material at http://link.aps.org/supplemental/10.1103/PhysRevB.92.094420 for examples of M vs T and inverse susceptibility measurements.

[23] K.-U. Neumann and K. R. A. Ziebeck, Arrott plots for rare earth alloys with crystal field splitting, J. Magn. Magn. Mater. **140-144**, 967 (1995).

[24] A. Arrott and J. E. Noakes, Approximate equation of state for nickel near its critical temperature, Phys. Rev. Lett. **19**, 786 (1967).

[25] I. Yeung, R. M. Roshko, and G. Williams, Arrott-plot criterion for ferromagnetism in disordered systems, Phys. Rev. B **34**, 3456 (1986).

[26] H. Luo, Q. Gibson, J. Krizan, and R. J. Cava, Ferromagnetism in Mn-doped Sb_2Te, J. Phys.: Condens. Matter **26**, 206002 (2014).

[27] R. S. Selinsky, D. J. Keavney, M. J. Bierman, and S. Jin, Element-specific magnetometry of EuS nanocrystals, Appl. Phys. Lett. **95**, 202501 (2009).